Analysis of MUSE-VLT observations of NGC 1365

Candidate number 15624
(Dated: October 18, 2024)

Using MUSE-VLT observational data of the NGC 1365 galaxy we first study the spectra of 3 regions in the galaxy where one is the nucleus and the two others are a bit further away. We find typical bright emission lines where Hα is the brightest and a flat continuum. We also study the emission maps of [OIII]*N$_2$ and Hα which show that the galaxy has a lot of star formation parallel to the bar of the galaxy and ionized outflows perpendicular to the bar. Velocity maps of Hα show a non-circular rotation of the ionized gas with the North-East part of the galaxy approaching us and the South-West part receding. We found the velocity dispersion to be largest where we also have a lot of outflows due to [OIII]$^*N_2$ emission.

I. INTRODUCTION

The NGC 1365 is a nearby Seyfert galaxy about 17 Mpc from us and it is an active star forming galaxy [1]. The main goals of this analysis is to study the ionized gas kinematics of NGC 1365 using mainly the bright optical emission lines [OIII]*N$_2$ and Hα.

In this report we will study observational data of the galaxy taken by the MUSE instrument on VLT. Explanations about the instrument and dataset is given in section II. First we will investigate three regions of the galaxy, study the spectra coming from these regions and differences between them. Then we will study the emission maps of Hα and [OIII]$^*N_2$ to see in which regions we have star formations and ionized outflows. Lastly we try to understand the ionized gas kinematics of the galaxy by studying momentum maps for Hα using BBarolo as a tool.

II. METHODS

MUSE (Multi Unit Spectroscopic Explorer) is an instrument on the Very Large Telescope (VLT) on the European Southern Observatory (ESO). It is an integral-field spectrograph operating in the wavelength range of visible light. It performs imaging and spectroscopy simultaneously and produces a spectrum for each pixel (spaxel) of the field of view. For our observation the wide field mode was used with a field of view covering 1'x1' [2].

For the analysis we used the file `ADP.2017-03-27T12_08_50.541.fits`, which contains the observational data and is a datacube of dimension (320, 317, 3682) pixels. The datacube stores the flux density as a 3D image where the first two dimensions are the spatial dimension of size (320, 317) pixels. The spatial dimension is the Ra and Dec of the data given in units of degrees. The last dimension of size 3682 pixels is the spectral dimension which is the wavelengths of the data given in ångström.

All relevant observational and technical parameters for this analysis is given in table II. The instrumental spatial resolution is 0.65", but since the observation is taken from Earth our data is affected by seeing. We therefore use the seeing limited spatial resolution corrected by airmass, 0.86". The field of view (FoV) is given in the header of the datacube as (320, 317) pixels which corresponds to 64" × 63.4" as the pixel size is 0.2".

Typical for an active star forming galaxy is that it usually has a lot of gas, a very rich interstellar medium and a high rate of star formation [3]. The lines that we expect to see in the sepctra of NGC 1365 are listed in the table below, table I. Because the universe is expanding the galaxy has a cosmological redshift of $z = 0.005476$ [1]. We use the redshift to calculate the expected observed wavelengths of emission lines in the spectra from the galaxy using the formula

$$\lambda_{obs} = (z + 1)\lambda_{rest} \tag{1}$$

where λ_{rest} is the rest frame wavelength and λ_{obs} is the expected observed wavelength.

Emission line	λ_{rest} [Å]	λ_{obs} [Å]
H$^*_\beta$	4861.3	4887.9
[OIII]*N$_1$	4958.9	4986.1
[OIII]*N$_2$	5006.8	5034.2
HeI	5875.6	5907.8
HeII	5977.0	6009.7
[OI]	6300.3	6334.8
Hα	6562.8	6598.7
[NII]*	6548.1	6584.0
[NII]*	6583.4	6619.5
[SII]*	6717.0	6753.8
[SII]*	67313.3	6768.2

Table I. Emission lines typically observed in star forming galaxies. The rest frame wavelengths are retrieved from lecture notes 8 [4] and λ_{obs} is calculated using formula 1.

Parameter	Value
Spatial resolution	0.65”
Spectral resolution at 5000 Å	1750 ± 4
Spectral resolution at 7000 Å	2737 ± 4
Seeing limited resolution	0.86″
FoV	64” × 63.4”
Pixel size	0.2”
Integration time	4000 s
Wavelength range	4750 - 9352 Å
Flux density units	$[10^{-20}$erg/s/cm^{2}Å$]$
Observation date	12th of October 2014
Observing time	12:06:24 UT

Table II. Important observational and technical parameters for this analysis. All parameters are retrieved from the header of the datacube except for the FoV as explained in section II and the spectral resolution retrieved from MUSE manual [5].

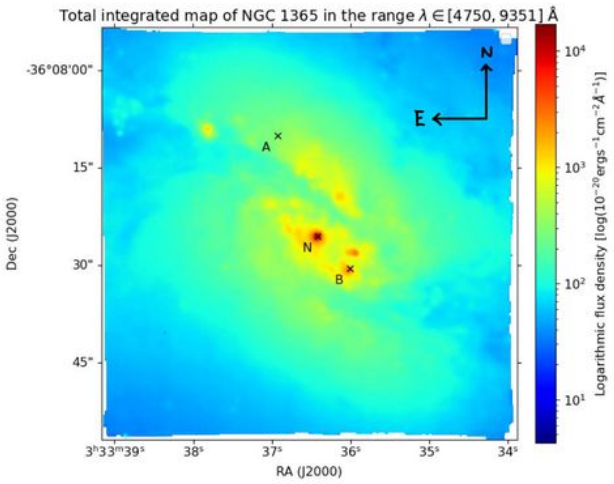

Figure 1. Total integrated map of the NGC 1365 galaxy created by integrating over the whole spectral range. The crosses mark the positions given in table III.

III. ANALYSIS AND RESULTS

A. Integrated map of source

We produce a total integrated map of the source by integrating the emission from the source over the entire spectral range which collapses all of the spectrum in one image. The integrated map we get is shown in figure 1. To emphasize the low surface brightness features, we used a logarithmic scaling.

The angular extent of this map is given by the field of view in table II as $64'' \times 63.4''$. This corresponds to a physical extent of 5.3 kpc as stated in the article by Venturi et al. [6]. From the image we see that NGC 1365 is a spiral galaxy with two main arms. The flux is highest at the center of the galaxy and decreases further away from the nucleus and the spiral arms.

B. Spectrum extraction

To study the spectra of the galaxy we use the software QFitsView [7]. We choose three positions N, A and B, where we want to study the spectra of the galaxy. These positions are marked in figure 1 and the respective coordinates are given in table III. We chose to study the spectra in these different positions to get a better idea of which parts of the galaxy reveals gas outflows, which parts are more dominated by star formations and how the gas moves in these regions. We therefore chose the nucleus, N, a position with a small offset from the nucleus, B and a position further a way, A.

Position	RA [J2000]	Dec [J2000]
N	$03^h33^m36''.435$	$-36°08'25''.68$
A	$03^h33^m36''.947$	$-36°08'08''.28$
B	$03^h33^m36''.022$	$-36°08'30''.68$

Table III. Coordinates of the 3 regions N, A and B where we study the spectra of the galaxy.

When extracting the spectra in these regions we use a circular aperture of 5 pixels wide to ensure that the source is resolved. As mentioned previously, the instrumental spatial resolution is 0.65”, but our data is affected by seeing which decreases the spatial resolution. The article by Venturi et. al [6] mentions that the average seeing is 0.76” for the Hα line [6], but in the header we found that the delivered seeing corrected by airmass was 0.86”. However, it does not say for which wavelength and since the spatial resolution depends on the wavelength, we use 5 pixels to ensure that the source is resolved considering the seeing limited resolution with highest value, 0.86”, and that the pixel size is 0.2”.

We export the wavelength value and corresponding flux values of the three regions to python and plot the entire spectra for the 3 positions N, A and B which are shown in figure 2, 3 and 4. From these figures we see that the most prominent lines appear in the wavelength ranges $\lambda \in [4800 - 5100]\mathring{A}$ and $\lambda \in [6500 - 6800]\mathring{A}$. We therefore zoom in on these ranges for each of the three positions. The dashed lines in all the spectra

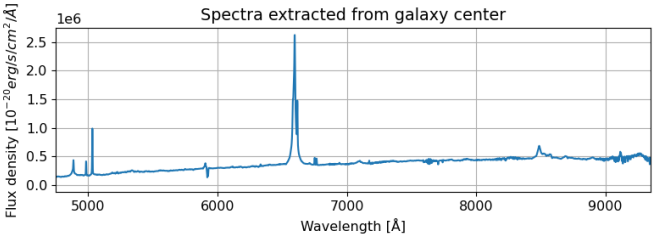

Figure 2. Spectrum of the whole wavelength range extracted from the center of the galaxy in region N.

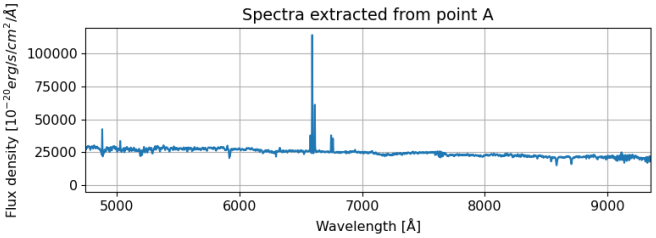

Figure 3. Spectrum of the whole wavelength range extracted from region A.

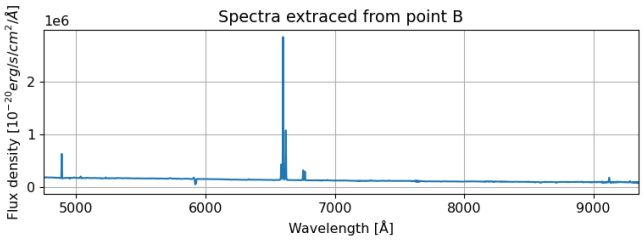

Figure 4. Spectrum of the whole wavelength range extracted from region B.

show values of expected λ_{obs} as listed in table I. For the zoomed in nucleus spectra given in figure 5 and 6 we see a total of 8 different emission lines slightly blueshifted compared to the estimated observed wavelengths listed in table I. We also see a broad Hα and Hβ line. The zoomed in spectra from position A shown in figure 7 and 8 show only 7 emission lines which are all narrow, where [OIII]$^*N_1$ is the one not visible. These lines are also blueshifted and the continuum is a bit noisier for A. In the last zoomed in spectra from region B given in figure 9 and 10 we see only 6 narrow lines, where [OIII]$^*N_1$ again is missing in addition to the [OIII]$^*N_2$ line which is so faint that we can not say for sure if it is there. The emission lines from region B are a bit redshifted.

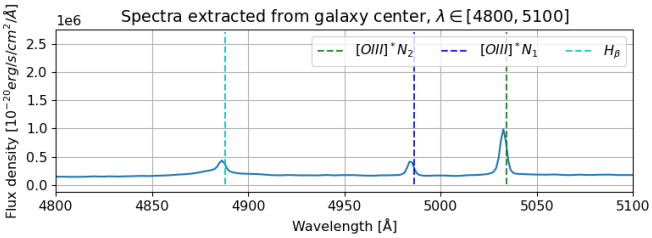

Figure 5. Spectrum extracted from the nucleus, N, with spectral range $\lambda \in [4800, 5100]$.

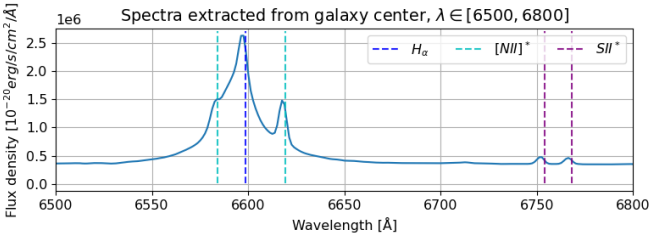

Figure 6. Spectrum extracted from the nucleus, N, with spectral range $\lambda \in [6500, 6800]$. Note that the sulfur lines should be forbidden, [SII]*.

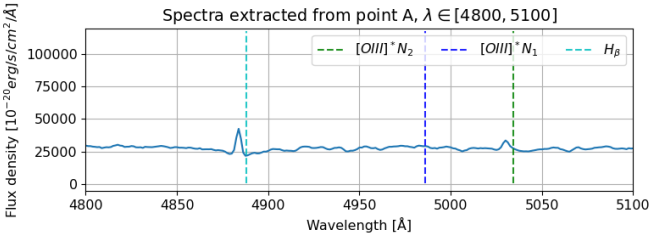

Figure 7. Spectrum extracted from region A with spectral range $\lambda \in [4800, 5100]$.

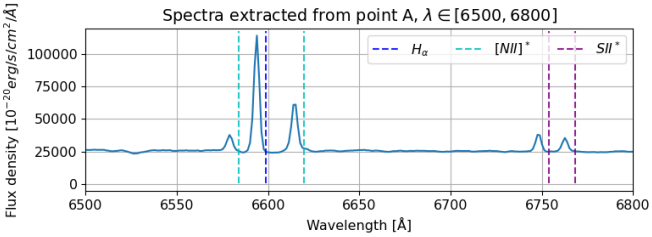

Figure 8. Spectrum extracted from region A with spectral range $\lambda \in [6500, 6800]$. Note that the sulfur lines should be forbidden, [SII]*.

C. Line emission map

To produce a map of the total [OIII]$^*N_2$ emission we use the spectrum in region N where the emission line is strong and narrow. In QFitsView we select the wavelength range $\lambda \in [5024, 5042]$ which captures the

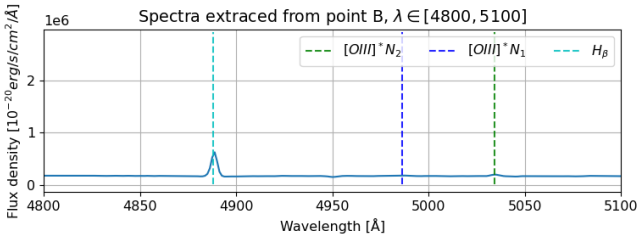

Figure 9. Spectrum extracted from region B with spectral range $\lambda \in [4800, 5100]$.

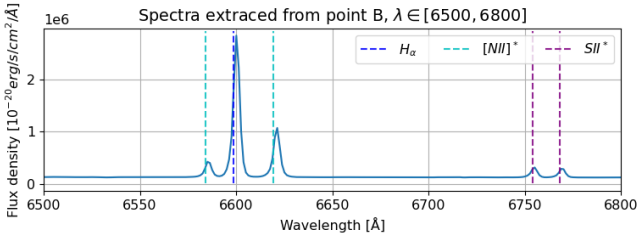

Figure 10. Spectrum extracted from region B with spectral range $\lambda \in [6500, 6800]$. Note that the sulfur lines should be forbidden, $[SII]^*$.

whole emission line and subtract the continuum om both sides of the line. We then integrate over the spectral range of the emission line to produce the emission map shown in figure 11. We repeat the same process to make a map of the total Hα emission, but this time we use the spectrum in region B where we have a more narrow and clear Hα emission line than in region N. We select the wavelength range $\lambda \in [6594, 6608]$ and again extract the continuum on both sides. The resulting plot is shown in figure 12.

For both line emission maps we calculate the noise level. This is done by first defining a square region where there is not much signal. This region is shown as a black square in the lower right corner in figure 11 and 12. We then compute the average 1σ RMS noise level by finding the standard deviation of the values in the square and over-plot the contours corresponding to 3σ, 10σ and 20σ on both emission line maps. The calculated noise levels are given in table IV.

Line map	**1σ**	**3σ**	**10σ**	**20σ**
Hα	12.66	37.98	126.61	253.22
$[OIII]^*N_2$	7.61	22.82	76.06	152.12

Table IV. Calculated standard deviations from the line emission maps. All the RMS-values have the same flux density units as given in table II.

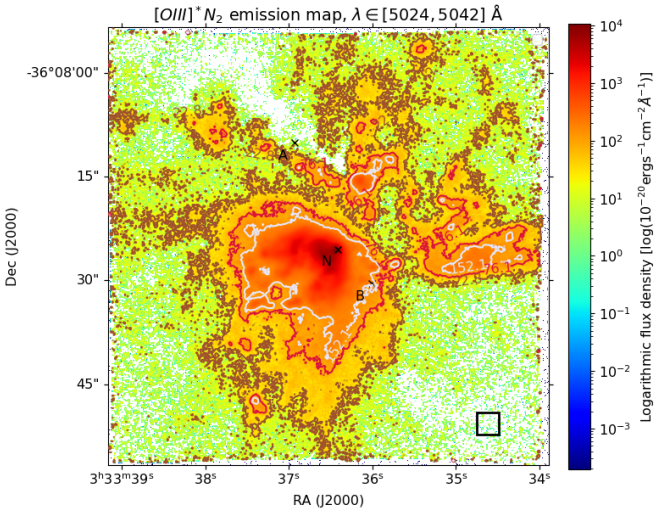

Figure 11. Map of the total $[OIII]^*N_2$ emission with continuum subtracted. The outer contour line in brown shows an RMS value of 3σ, red shows 10σ and white shows 20σ.

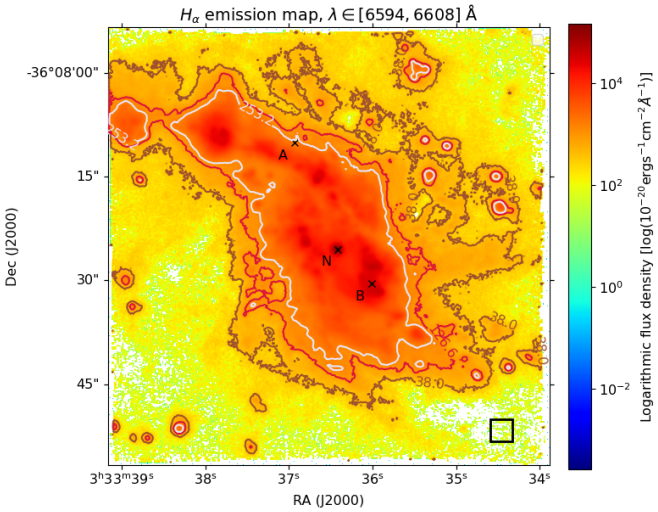

Figure 12. Map of the total Hα emission with continuum subtracted. The outer contour line in brown shows an RMS value of 3σ, red shows 10σ and white shows 20σ.

D. Gas kinematics

To study the gas kinematics of the galaxy we use BBarolo as a tool. First we prepare a datacube of the Hα line we want to study by cutting the datacube around this emission line. We try different wavelength ranges and find that the range that best covers the line is a wavelength range of $\lambda \in [6590, 6607]$. We choose Hα because it is the brightest line in the spectrum to maximize S/N. Then we give the prepared datacube to BBarolo together with a parameter file. In the parameter file we include the inclination of 40° [6], the distance to the galaxy of 17.3 Mpc [6], the redshift $z = 0.005476$, the spectral resolution and the wavelength in the restframe for Hα found in table I.

The momentum maps we get from BBarolo is shown in figure 13. The images on the left side show the data we gave BBarolo, the images in the middle show the model fitted to the data and the images on the right show the residuals. The top three images are momentum 0 maps or intensity maps which are the integrated flux across the spectral range of the $H\alpha$ line. The middle row of images show momentum 1 maps or velocity maps which are the integrated velocity times the flux, normalized by the flux. The units are the average velocity of each pixel. We see that one part of the velocity map is redshifted and the other part is blueshifted. The bottom row of images show momentum 2 maps or dispersion maps which is the velocity dispersion of each pixel. We see a peak of dispersion around the center of the galaxy.

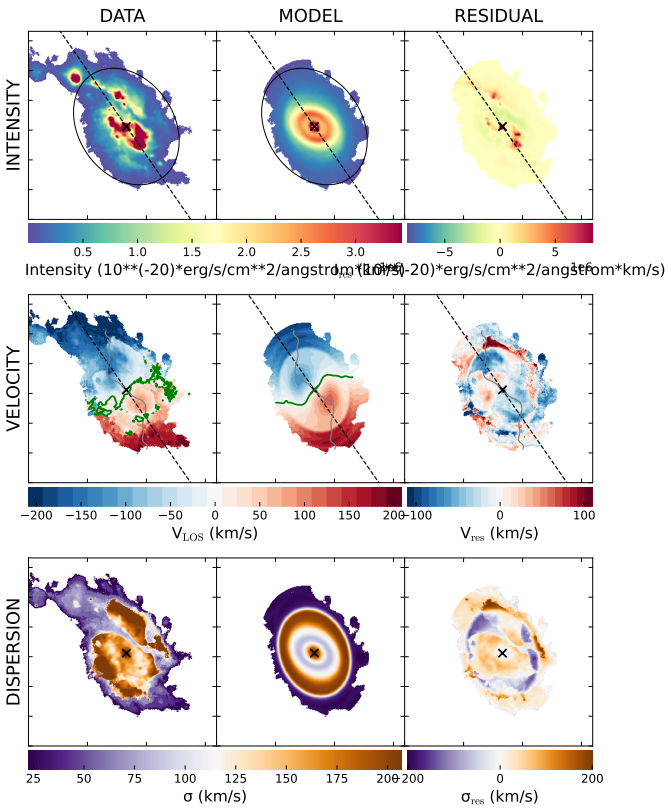

Figure 13. Intensity map (top), velocity map (middle) and dispersion map (bottom) of Hα line constructed with 3D BBarolo. The major axis is shown as a dashed line in the top and middle images.

IV. DISCUSSION

A. Integrated map of source

From the integrated map of the galaxy seen in figure 1 we see that that the galaxy is a spiral galaxy with two arms. The galaxy seems to have a bar spanning in a direction parallel to the line between region N to B. The nucleus of the galaxy has the highest flux values, but we also see some small regions along the central bar of the galaxy with very high flux values. Region B is one of the high flux regions and these high values might indicate the presence of bright optical star clusters. It has in fact been proven that there are optical super star clusters in the region around B by Kristen et al. [8].

B. Spectrum extraction

We see as expected for an active star forming galaxy that the emission lines are quite bright compared to the continuum which is low and flat. This means that there are not many stellar absorption lines and we see only a few ones which might be due to the source, but also might be due to absorption in Earth's atmosphere [3]. Even though the spectra are supposed to be corrected for telluric absorption there are some residual telluric lines. These are however only shown in the whole spectra in figure 2, 3 and 4 and not very prominent. In the zoomed in spectra we do not see any absorption lines. We see many of the emission lines expected from an active star forming galaxy listed in table I. The brightest ones are Hα, [NII]* and [OIII]*N_2. We do not observe HeI or HeII as they are not in the zoomed in regions and to small to be found on any of the the whole spectra.

In the spectra from the nucleus, shown in figure 5 and 6, we have broader Balmer lines than in the spectra from region A and B. The reason for this is that the gas is moving at a high velocity around the black hole at the center of the galaxy creating a doppler shift in both directions which results in a doppler broadening. We also see that the spectra from the nucleus and region B have a much stronger Hα and Hβ line than region A which indicate a much higher rate of star formation in these regions. The fact that region B is dominant by

super star clusters as mentioned previously causes the Hα line in region B to be very strong. Since the Hα and Hβ lines are clearly visible in all three regions, it is clear that the galaxy must indeed be a star forming galaxy. The [OIII]*N$_2$, which is present in the nucleus, in region A and just barely in region B, indicate ionized outflows in these regions which is common for active galactic nuclei [6]. The [SII]* lines are present in all regions which is also typical for an active star forming galaxy [3]. The different emission line ratios in the three spectra indicate different ionization mechanisms in each of the different regions.

We see that the lines from the nucleus are a little bit blueshifted and the lines from region A are even more blueshifted. The lines from region B are on the other hand a little bit redshifted. This indicated that the gas in the nucleus and especially region A are moving away from us while the gas in region B is moving towards us.

In further studies of the galaxy with this data we could for example have studied the electron density from the line ratio of the [SII]* lines which are clearly visible in all our spectra as done in Venturi et. al [6].

C. Line emission map

When estimating the noise level of the maps we see that the RMS value is bigger for the Hα emission map than for the oxygen emission map. We know that the noise level depends on the integration time, and also on the spectral width that we use to integrate the map. If we use data from a larger spectral width the noise will decrease according to the radiometer equation $S/N = \sqrt{\Delta t \Delta \nu}$. Since the integration time is constant it does not contribute to a difference in the RMS values. We see that the the oxygen emission line is integrated over a larger spectral range making the signal to noise ratio higher and therefore the noise level lower for this line than for the Hα line. The RMS value also depend on several other factors, like how well we managed to extract the continuum and which region on the emission maps we choose to calculate the noise level.

A point on the emission map is considered to be part of the signal if its value is bigger than 3σ meaning that the area within the brown contour lines in figure 11 and 12 is considered as signal. We see that the region where we have a flux value above 20σ is smaller for the oxygen map than for the Hα map. The two maps also have different spatial distributions. Hα dominates in an elongated region which spans from the North-East to the South-West of the image, parallel to the bar, while [OIII]*N$_2$ emission is more prominent in a direction perpendicular to the one of Hα, with most emission in the region from the nucleus towards South-West. This suggests that we have a star forming region parallel to the galaxy bar with some additional smaller regions with strong Hα emission also indicating stellar formation, while perpendicular to the bar we have a region with ionized outflows. This is consistent with what was found by Venturi at. al [6].

To better estimate where we are sure to have a detectable signal and how strong the signal is in these regions, we could have calculated the signal to noise ratio of each line by dividing the peak flux value of the line by the calculated standard deviation. A value of S/N above 3, or even better, 5 means that we have a certain detection and we could have excluded spaxels having a S/N lower than 3 for a more representative map of the line emissions. To improve the S/N-ratio and also our emission maps we could have done a Gaussian fit of the line profile to better calculate the peak flux value and improve the signal quality.

D. Gas kinematics

We chose to study the velocity of Hα as the ionized gas kinematics can be easier studied from the velocity of this emission due to the fact that the profile of Balmer lines is less affected by outflow as stated in the article by Venturi et. al [6]. On the images in the middle row of figure 13 we see that one side of the galaxy is redshifted and moving away from us while the other side is blueshifted and moving towards us. This tells us that the galaxy is rotating. This is consistent with what what we found about the shifts of the emission lines in the spectra of positions N, A and B. We saw that the emission lines in A was much more blueshifted than B was redshifted which we see is because the gas in position A is approaching us faster than the gas in position B is moving away from us. This is also consistent with what was found in the article by Venturi et. al. [6]. If we look at the image on the right of the velocity map we see that we have a significant amount of residual. This might be due to the fact that BBarolo forces the data into a circular rotation pattern, and non-circular motion like outflows are then not fully reproduced in the model. We can therefore see that the the gas is not rotating in a perfect circular motion but is affected by outflows which we know is true due to the precence of [OIII]*N$_2$. We also note a twisted Z shape of the boundary where the velocity changes sign marked in green in figure 13. This shape is likely due to the bar in the galaxy.

We see a peak in the dispersion diagram around the center of rotation likely due to the supermassive black hole in the nucleus of the galaxy. The dispersion map also show some broader features which may be due to the fact that astronomical objects do not follow

perfect disks, but there could be other processes that lead to perturbations in the kinematics. We see in the bottom left image in figure 13 that the places with highest value of dispersion is the same places where we found [OIII]*N_2 emission. It is therefore probable that the large dispersion in these areas are due to the ionized outflows in the same regions.

We did not reduce the noise in any way when we cut the datacube before using it with the BBarolo software which might have affected the resulting momentum maps in figure 13. Had we subtracted the continuum or reduced the noise in other ways we might have gotten a better model fit, especially for the velocity dispersion map which we see does not do a very good job at modeling the data. The model of the intensity map is not very good either, but that one we have studied previously.

V. CONCLUSION

The galaxy NGC 1365 is a star forming galaxy which we have seen have spectra typical for this type of galaxy. The spectra from both the nucleus and regions further away all show bright emission lines with a flat continuum. The spectra show broader Balmer lines in the nucleus due to gas at high velocity and otherwise narrow lines. From emission maps of Hα and [OIII]*N_2 we see that the region parallel to the bar has a lot of star formation due to Hα being most prominent here and that the region perpendicular to the bar, especially in the South-East direction has a lot of ionized outflows due to [OIII]*N_2 emission. From studying the momentum maps of Hα we see that the gas in the galaxy has a non-circular rotation pattern. The velocity maps show that gas in the North-East part of the galaxy is blueshifted while the gas in the South-West region is redshifted which is consistent with what the spectra from different locations in the galaxy showed. We also found that the velocity dispersion is largest where we also have a lot of outflows due to [OIII]*N_2 emission.

[1] M. Wenger, F. Ochsenbein, D. Egret, P. Dubois, F. Bonnarel, S. Borde, F. Genova, G. Jasniewicz, S. Laloë, S. Lesteven, and R. Monier, **143**, 9 (2000), arXiv:astro-ph/0002110 [astro-ph].

[2] E. S. Observatory, "A multi unit spectroscopic explorer - muse," .

[3] C. Cicone, "Spectroscopy and integral field unit observations," University Lecture (2023).

[4] C. Cicone, *Spectroscopy and IFUs* (Institute of Theoretical Astrophysics, UiO, 2022).

[5] R. J., R. Bacon, and J. Vernet, "Muse user manual," .

[6] G. Venturi, E. Nardini, A. Marconi, S. Carniani, M. Mingozzi, G. Cresci, F. Mannucci, G. Risaliti, R. Maiolino, B. Balmaverde, A. Bongiorno, M. Brusa, A. Capetti, C. Cicone, S. Ciroi, C. Feruglio, F. Fiore, A. Gallazzi, F. La Franca, V. Mainieri, K. Matsuoka, T. Nagao, M. Perna, E. Piconcelli, E. Sani, P. Tozzi, and S. Zibetti, **619**, A74 (2018), arXiv:1809.01206 [astro-ph.GA].

[7] T. Ott, "Qfitsview," (2021).

[8] H. Kristen, S. Jorsater, P. O. Lindblad, and A. Boksenberg, **328**, 483 (1997).